



1 **Quantifying streamflow and active groundwater storage in response to climate**

2 **warming in an alpine catchment on the Tibetan Plateau**

3 Lu Lin^{a,b}, Man Gao^c, Jintao Liu^{a,b*}, Xi Chen^{a,b,c}, Hu Liu^d

4 ^a *State Key Laboratory of Hydrology-Water Resources and Hydraulic Engineering,*
5 *Hohai University, Nanjing 210098, People's Republic of China*

6 ^b *College of Hydrology and Water Resources, Hohai University, Nanjing 210098,*
7 *People's Republic of China*

8 ^c *Institute of Surface-Earth System Science, Tianjin University, Tianjin 300072, People's*
9 *Republic of China*

10 ^d *Linze Inland River Basin Research Station, Chinese Ecosystem Research Network,*
11 *Lanzhou 730000, People's Republic of China*

12 * *Corresponding author. Tel.: +86-025-83787803; Fax: +86-025-83786606.*

13 *E-mail address: jtliu@hhu.edu.cn (J.T. Liu).*

14



15 **Abstract**

16 Climate warming is changing streamflow regimes and groundwater storage in cold
17 alpine regions. In this study, a headwater catchment named Yangbajain in the Lhasa
18 River basin on the Tibetan Plateau is adopted as the study area for quantifying
19 streamflow changes and active groundwater storage in response to climate warming.
20 The catchment is characterized by alpine glacier and frozen ground which covers about
21 11% and 86% of the total area, respectively. The changes in streamflow regimes
22 (including quickflow and baseflow) and climate factors are evaluated based on hydro-
23 meteorological observations from 1979 to 2013. Then active groundwater storage in
24 autumn and early winter is quantified by recession flow analysis assuming
25 nonlinearized outflow from aquifers into streams. The results show that annual
26 streamflow increases significantly at a rate of about 12.30 mm/10a during this period.
27 The significant increase of annual air temperature compared with nonsignificant
28 variation of annual precipitation indicates that the climate warming takes
29 responsibilities to the increase of streamflow. It is believed that the increased
30 streamflow is mainly fed by glacier meltwater, which has led to over 25% loss of the
31 total glacial volume in the past 50 years (1960-2009) in this catchment. Moreover, the
32 significant increase of annual baseflow at a rate of about 10.95 mm/10a is the dominant
33 factor for the increase of the total streamflow. Through recession flow analysis, we find
34 that recession coefficient K and active groundwater storage S in autumn and early
35 winter increase significantly at the rates of about 7.70 ($\text{mm}^{0.79}\text{d}^{-0.21}$)/10a and 19.32



36 mm/10a during these years. The increase of active groundwater storage can partly be
37 explained by frozen ground degradation, which lead to the enlargement of groundwater
38 storage capacity and accommodate more summer rainfall and meltwater in the wide
39 and flat valley, and then slowly release them into streams in the following seasons. Thus,
40 it is reasonable to attribute the increase of baseflow and the slowdown of baseflow
41 recession process in autumn and early winter to the enlargement of groundwater storage
42 capacity. Through quantifying streamflow changes and active groundwater storage in
43 response to warming-induced changes, this study provides a perspective to clarify the
44 way of glacial retreat and frozen ground degradation on hydrological processes.

45 **Keywords:** Climate warming; Streamflow; Groundwater storage; Glacier retreat;
46 Frozen ground degradation; Tibetan Plateau

47 **1. Introduction**

48 Often referred to as the “Water Tower of Asia”, the Tibetan Plateau (TP) is the source
49 area of major rivers in Asia, e.g., the Yellow, Yangtze, Mekong, Salween, Indus, and
50 Brahmaputra Rivers (Cuo et al., 2014). The delayed release of water resources on the
51 TP through glacier melt can augment river runoff during dry periods as a pivotal role
52 for water supply for downstream populations, agriculture and industries in these rivers
53 (Viviroli et al., 2007; Pritchard, 2017). However, the TP is experiencing a significant
54 warming trend during the last half century (Kang et al., 2010; Liu and Chen, 2000).
55 Along with the rising temperature, major warming-induced changes have occurred over
56 the TP, such as glacier retreat (Yao et al., 2004; Yao et al., 2007) and frozen ground



57 degradation (Wu and Zhang, 2008). Hence, it is of great importance to elucidate how
58 climate warming influences hydrological processes and water resources on the TP.

59 In cold alpine catchments, glacier is known as “solid reservoir” that supplies water
60 as streamflow, while frozen ground, especially permafrost, serves as an impermeable
61 barrier to the interaction between surface water and groundwater (Immerzeel et al.,
62 2010; Walvoord and Kurylyk, 2016). Since the 1990s, most glaciers across the TP have
63 retreated rapidly due to global warming and caused an increase of more than 5.5% in
64 river runoff from the plateau (Yao et al., 2007). Meltwater is the key contributor to
65 streamflow increase especially for headwater catchments with larger glacier coverage
66 (>5%) (Bibi et al., 2018). Meanwhile, in a warming climate, numerous studies
67 suggested that frozen ground on the TP has experienced a noticeable degradation during
68 the past decades (Cheng and Wu, 2007; Wu and Zhang, 2008). Frozen ground
69 degradation can modify surface conditions and change thawed active layer storage
70 capacity in the alpine catchments (Niu et al., 2011). Thawing of frozen ground increases
71 surface water infiltration, supports deeper groundwater flow paths, and then enlarges
72 groundwater storage, which is expected to have a profound effect on flow regimes
73 (Bense et al., 2009; Bense et al., 2012; Walvoord and Striegl, 2007; Woo et al., 2008;
74 Ge et al., 2011; Walvoord and Kurylyk, 2016). In cold alpine catchments where large
75 areas of glacier and frozen ground exist, warming-induced glacier and frozen ground
76 co-variations fundamentally affect the water supply and the mechanisms of streamflow
77 generation and change (Cuo et al., 2014; Pritchard, 2017).



78 It is challenging to understand how glacier melt and frozen ground thaw alters the
79 mechanism of streamflow in a warmer climate due to the complicated interactions
80 between hydrological and cryospheric processes. In earlier phase of glacier melt,
81 accelerated glacier retreat will bring large quantities of meltwater available directly for
82 surface runoff or indirectly for groundwater recharge (Bayard et al., 2005). Meanwhile,
83 frozen ground thawing may allow for increased groundwater recharge from meltwater
84 infiltration (Evans and Ge, 2017). Generally, climate warming is hypothesized to
85 generate a quantitative and temporal shift in the partitioning of meltwater between
86 surface runoff and groundwater flow, and thereby alter the quantity and timing of
87 baseflow (Green et al., 2011; Evans et al., 2018). Evans et al. (2015) found that an
88 increase in mean annual surface temperature of 2°C reduced approximately 28% areal
89 extent of permafrost and tripled baseflow contribution to streamflow using a physically
90 based groundwater model in a headwater catchment of the Heihe River on the northern
91 TP. Qin et al. (2016) discovered that the increasing precipitation and the thawing of
92 frozen ground were the main factors on the increase of baseflow with no significant
93 change in surface runoff in the upper Heihe River basin of the northeastern TP. Previous
94 data-based studies indicated that the baseflow has increased especially during winter
95 with a reduction or no pervasive change in summer streamflow in the central and
96 northern TP (Liu et al., 2011; Niu et al., 2016) as well as the Arctic rivers (Walvoord
97 and Striegl, 2007; Smith et al., 2007; St. Jacques and Sauchyn, 2009). Moreover, Bense
98 et al. (2012) suggested that the increasing groundwater storage caused by frozen ground



99 degradation would delay baseflow increase possibly by several decades to centuries
100 based on numerical simulations. The slowdown in baseflow recession processes was
101 found in the northeastern and central TP (Niu et al., 2011; Niu et al., 2016; Wang et al.,
102 2017), in northeastern China (Duan et al., 2017), and in Arctic rivers (Lyon et al., 2009;
103 Lyon and Destouni, 2010; Walvoord and Kurylyk, 2016).

104 While, previous qualitatively studies were important for understanding the effects of
105 climate warming on hydrological changes in cold alpine catchments (Niu et al., 2011;
106 Niu et al., 2016; Wang et al., 2017). However, quantitatively characterizing storage
107 properties and sensitivity to climate warming in cold alpine catchments is important for
108 local water as well as downstream water management (Staudinger, 2017). Moreover,
109 revealing the storage characteristics makes it easier to predict hydrological cycle and
110 streamflow changes response to warming climate in cold alpine catchments (Singleton
111 and Moran, 2010). Thus, this study focuses on quantifying streamflow and aquifer
112 storage volume response to changes in glacier melt and frozen ground thaw at
113 catchment scale on the southern TP. Given the difficulty of direct measurements for
114 catchment aquifer storage (Staudinger, 2017; Käser and Hunkeler, 2016) and low
115 spatial resolution for the GRACE satellites to assess total groundwater storage changes
116 at catchment scale (Green et al., 2011), an alternative method, namely, recession flow
117 analysis, can be theoretically used to derive the active groundwater storage volume in
118 the phreatic aquifer to reflect frozen ground degradation in a catchment (Brutsaert and
119 Nieber, 1977; Brutsaert et al., 2008). For example, the groundwater storage changes



120 have been inferred by recession flow analysis assuming linearized outflow from
121 aquifers into streams (Lin and Yeh, 2017). However, the non-linear of the storage
122 discharge relationship dominates baseflow recession processes for most catchments due
123 to the complex structures and properties of catchment aquifers (Chapman, 1999; Liu et
124 al., 2016). Moreover, groundwater storage computed by assuming the aquifers as linear
125 reservoir cannot reflect the actual storage (Wittenberg, 1999). Lyon et al. (2009)
126 adopted the non-linear reservoir to fit flow recession curves for derivation of aquifer
127 attributes, which can be developed for inferring aquifer storage. Buttle (2017) used
128 Kirchner (2009) approach for estimating dynamic storage in different basins and found
129 that storage and release of dynamic storage may mediate baseflow response to temporal
130 changes.

131 In this study, the long-term changes in streamflow and climate factors in a glacier-
132 fed headwater catchment with frozen ground in the Lhasa River basin of the south-
133 central TP is analyzed using non-parametric tests during the period 1979-2013. The
134 First and Second Glacier Inventory of China is used to assess the response of glacier
135 variations to climate warming. Changes in streamflow components, baseflow recession
136 process and active groundwater storage are examined. The main objectives of this study
137 are (1) to identify the water source for streamflow changes in climate warming; (2) to
138 discuss the water volume changes in the partitioning between surface runoff and
139 groundwater flow due to changes in glacier melt and frozen ground thaw; (3) to quantify
140 active groundwater storage volume by recession flow analysis assuming nonlinearized



141 outflow from aquifers into streams, and to analyze the impacts of the changes in active
142 groundwater storage on streamflow variation.

143 **2. Materials and Methods**

144 **2.1. Study area**

145 Located on the south-central TP, the Yangbajain catchment is a glacier-fed headwater
146 catchment with highly frozen ground coverage in the western part of the Lhasa River
147 Basin (Figure 1a). The catchment has an area of approximately 2,645 km² and its
148 elevations range from 4,270 to 6,400 m (Figure 1b). In the east of the catchment, the
149 wide and flat valley (Figure 1b) is located in the Damxung-Yangbajain fault of the
150 southeastern piedmont of Nyainqêntanglha Mountains (Jiang et al., 2016; Yang et al.,
151 2017) with low-lying flat terrain and thicker aquifers due to the great thickness
152 quaternary loose sediment (Wu and Zhao, 2006). The coverage of glacier area is about
153 11% in the catchment, which is the highest glacierized sub-catchment in the Lhasa
154 River Basin. The total glacier area was about 316.31 km² in 1960 according to the First
155 Chinese Glacier Inventory (Mi et al., 2002) and most glaciers were found along the
156 Nyainqêntanglha Mountains range (Figure 1c). The ablation period of the glaciers
157 ranges from June to September with the glacier termini at about 5,200 m (Liu et al.,
158 2011). According to the new map of permafrost distribution on the TP (Zou et al., 2017),
159 the wide and flat valley is underlain by seasonally frozen ground (Figure 1c). It is
160 estimated that seasonally frozen ground and permafrost accounts for about 64% and 22%
161 of the total catchment area, respectively. The lower limit of alpine permafrost is around



162 4,800 m, and the thickness of permafrost varies from 5 m to 100 m (Zhou et al., 2000).

163 The climate in the catchment is characterized by semi-arid temperate monsoon
164 climate. The average annual air temperature of the Yangbajain catchment is
165 approximately -2.3°C with monthly variation from -8.6°C in January to 3.1°C in July
166 (Figure 2). The average annual precipitation at the Yangbajain station (4,305 m) in the
167 valley is about 427 mm. The intra-annual distribution of precipitation is extremely
168 uneven due to the pronounced rainy season during the summer monsoon (June-August)
169 and the dry season lasting the rest of the year. Nearly 73% of the total precipitation
170 occurs in summer, while only 1% of the precipitation occurs in winter (December-
171 February) (Figure 2).

172 The average annual runoff depth is 277.7 mm, and the intra-annual distribution of
173 streamflow is uneven. Approximately 63% of the annual streamflow is observed in
174 summer, whereas in the winter season, streamflow is low and accounts for only 4% of
175 the annual streamflow (Figure 2). Streamflow is recharged mainly by monsoon rainfall
176 and summer meltwater. The river in winter is only recharged by groundwater, which is
177 greatly affected by the freeze-thaw cycle of frozen ground and the active layer (Liu et
178 al., 2011).

179 **2.2. Data**

180 Daily streamflow and precipitation data at the Yangbajain station (4,305 m) during
181 the period 1979-2013 are collected from Tibet Autonomous Region Hydrology and
182 Water Resources Survey Bureau. The monthly meteorological data at the Damxung



183 station (4,289 m), which is neighbor to the Yangbajain catchment (Figure 1a), are
184 obtained from the China Meteorological Data Sharing Service System
185 (<http://data.cma.cn/>) for the years from 1979 to 2013. In this study, the method of
186 meteorological data extrapolation by Prasch et al. (2013) is adopted to obtain the
187 discretized air temperature (with cell size as 1 km×1 km) of the Yangbajain catchment
188 based on the air temperature of the Damxung station assuming a linear lapse rate. The
189 mean monthly lapse rate is set to 0.44 °C 100 m⁻¹ with elevation below 4,965 m and
190 0.78 °C 100 m⁻¹ with elevation above 4,965 m in the catchment (Wang et al., 2015).

191 The glacier and frozen ground data are provided by the Cold and Arid Regions
192 Science Data Center at Lanzhou (<http://westdc.westgis.ac.cn/>). The distribution, area
193 and volume of glacier are based on the First and Second Chinese Glacier Inventory in
194 1960 and 2009. The distribution and classification of frozen ground are collected from
195 a new map of permafrost distribution on the Tibetan Plateau (Zou et al., 2017).

196 **2.3. Methods**

197 *2.3.1. Mann-Kendall test with trend free pre-whitening*

198 The Mann-Kendall (MK) test is applied to detect trends of hydro-meteorological time
199 series, which is robust against outliers and is suitable for data with non-normally
200 distributed or non-linear trends (Mann, 1945; Kendall, 1975). To remove the serial
201 correlation from the examined time series, a Trend-Free Pre-Whitening (TFPW)
202 procedure is needed prior to applying the MK test (Yue et al., 2002). A more detailed
203 description of the Trend-Free Pre-Whitening (TFPW) approach was provided by Yue



204 et al. (2002).

205 The MK test statistic s is calculated as

$$206 \quad s = \sum_{i=1}^{n-1} \sum_{j=i+1}^n \operatorname{sgn}(x_j - x_i) \quad (1)$$

207 where, x_j and x_i are the data values in sequence, n is the sequence length, and $\operatorname{sgn}(x_j -$

208 $x_i)$ are recorded as

$$209 \quad \operatorname{sgn}(x_j - x_i) = \begin{cases} 1, & x_j > x_i \\ 0, & x_j = x_i \\ -1, & x_j < x_i \end{cases} \quad (2)$$

210 The variance of s is proposed by the equation (3)

$$211 \quad \operatorname{Var}(s) = \frac{n(n-1)(2n+5)}{18} \quad (3)$$

212 Then, the standardized test statistic Z_C can be transformed from statistical value s ,

213 and is computed by equation (4)

$$214 \quad Z_C = \begin{cases} \frac{s-1}{\sqrt{\operatorname{Var}(s)}} & s > 0 \\ 0 & s = 0 \\ \frac{s+1}{\sqrt{\operatorname{Var}(s)}} & s < 0 \end{cases} \quad (4)$$

215 When $|Z_C| \leq 1.96$, there is no significant trend. The trend is at the 5% significance

216 level if $|Z_C| > 1.96$, and at the 1% significance level if $|Z_C| > 2.58$. A positive value of

217 Z_C indicates an upward trend, whereas a negative value indicates a downward trend in

218 the tested time series.

219 The trend magnitude is computed by Theil-Sen estimator (Sen, 1968)

$$220 \quad \beta = \operatorname{median} \left(\frac{x_i - x_j}{i - j} \right), \forall j < i \quad (5)$$



221 where $1 < j < i < n$, a positive value of β indicates an upward trend, and a negative value
222 indicates a downward trend.

223 2.3.2. Baseflow separation

224 In this paper, the most widely used one-parameter digital filtering algorithms is
225 adopted for baseflow separation (Lyne and Hollick, 1979). The first filter equation is
226 expressed as

$$227 \quad q_t = \alpha q_{t-1} + \frac{1+\alpha}{2} (Q_t - Q_{t-1}) \quad (6)$$

$$228 \quad b_t = Q_t - q_t \quad (7)$$

229 where q_t and q_{t-1} are the filtered quickflow at time step t and $t-1$, respectively; Q_t and
230 Q_{t-1} are the total runoff at time step t and $t-1$; b_t is the filtered baseflow. α is the filter
231 parameter, ranging from 0.9 to 0.95.

232 2.3.3. Determination of active groundwater storage

233 The method of recession flow analysis is widely used to investigate the baseflow
234 recession characteristics and the storage discharge relationship of catchments (Gao et
235 al., 2017). Physical considerations based on hydraulic groundwater theory suggest that
236 the groundwater storage in a catchment can be approximated as a power function of
237 baseflow rate at the catchment outlet (Brutsaert, 2008)

$$238 \quad S = Ky^m \quad (8)$$

239 where y is the rate of baseflow in the stream in a catchment, S is the volume of active
240 groundwater storage in the catchment aquifers (see in Figure 3), abbreviated as
241 groundwater storage in the following context. And K and m are constants depending on



242 the catchment physical characteristics. K represents the time scale of the catchment
243 streamflow recession process, commonly referred to as baseflow recession coefficient.

244 During a period without precipitation and evapotranspiration, the flow in a stream
245 can be assumed to depend solely on the groundwater storage from the upstream aquifers.
246 For such baseflow conditions, the conservation of mass equation can be represented as

$$247 \quad \frac{dS}{dt} = -y \quad (9)$$

248 where t is the time. Substitution of equation (8) in equation (9) yields

$$249 \quad -\frac{dy}{dt} = ay^b \quad (10)$$

250 where dy/dt is the temporal change of the baseflow rate during recessions, and the
251 constants a and b are called the recession intercept and recession slope of plots of $-dy/dt$
252 versus y in log-log space, respectively. The parameters of K and m in equation (8) can
253 be expressed by a and b , where $K = 1/[a(2-b)]$ and $m = 2-b$. In the storage
254 discharge relationship, the aquifer responds as a linear reservoir if $b=1$, and as non-
255 linear reservoir if $b \neq 1$.

256 In our study, the baseflow recession data are selected from the streamflow
257 hydrographs, which remarkably decline for at least 3 days after rainfall ceases and
258 remove the first 2 days to avoid the impact of storm flow (Brutsaert and Lopez, 1998).
259 A variable time interval Δt is used to properly scale the observed drop in streamflow to
260 avoid discretization errors on $-dy/dt \sim y$ plot due to measurement noise, especially in the
261 log-log space (Rupp and Selker, 2006; Kirchner, 2009). Meanwhile, the difference of
262 baseflow Δy in the catchment exceeds a critical precision threshold Δy_{crit} of 0.02



263 mm/day. Then the constants a and b are fit by using a non-linear least squares through
264 all data points of $-dy/dt$ versus y in log-log space for all years (1979-2013) to avoid the
265 difficulty of defining a lower envelop of the scattered points (Lyon et al., 2009). With
266 the fixed slope b during recessions (i.e., $b \neq 1$ remains constant), it should be possible to
267 observe changes in catchment aquifer properties by fitting the intercept a as a variable
268 across different years. Since the values of K and m for each year can be calculated by
269 fitting recession intercept a and the fixed slope b , the groundwater storage S in a
270 catchment is obtained through equation (8) based on average rate of baseflow during
271 recessions.

272 **3. Results and Discussion**

273 **3.1. Variation of annual streamflow and its components**

274 The annual streamflow of the Yangbajain catchment shows an increasing trend at the
275 5% significance level with a mean rate of about 12.30 mm/10a over the period 1979-
276 2013 (Table 1 and Figure 4a). Meanwhile, annual mean air temperature exhibits an
277 increasing trend at the 1% significance level with a mean rate of about 0.28 °C/10a
278 (Table 1 and Figure 5a). However, annual precipitation has nonsignificant trend during
279 this period (Table 1 and Figure 5b). The similar variation trends between annual
280 streamflow and annual air temperature indicate that the changes of air temperature may
281 act as a primary climatic factor for streamflow increase.

282 As the significant rising of air temperature, glacier in the catchment has been
283 retreating continuously. According to the twice Chinese Glacier Inventory (I & II



284 volume) in 1960 and 2009, the total glacial area and volume have decreased by 38.06
285 km² (12.0%) and 0.47×10¹⁰ m³ (26.2%) over the past 50 years (Figure 6). With the
286 nonsignificant increase of annual precipitation, it is reasonable to attribute annual
287 streamflow increase to the accelerated glacier retreat as the consequence of increasing
288 annual air temperature. This conclusion is also consistent with previous results by
289 Prasad et al. (2013), who suggested that glacial meltwater contribution to streamflow
290 would remain increase in the Yangbajain catchment together with significant increase
291 in streamflow and nonsignificant trend in precipitation by quantifying present and
292 future glacier meltwater contribution to runoff.

293 Overall, the annual mean baseflow contributes about 59% of annual mean
294 streamflow in the catchment through baseflow separation method. As annual
295 streamflow increases significantly, it is necessary to analyze to what extent the changes
296 in two streamflow components lead to streamflow increase. The result shows that
297 annual baseflow exhibits a significant increasing trend at the 1% level with a mean rate
298 of about 10.95 mm/10a over the period 1979-2013 (Table 1 and Figure 4b). This trend
299 is statistically nonsignificant for annual quickflow during the period (Table 1). Thus,
300 the increase in baseflow is the main contributor to streamflow increase. It can be further
301 concluded that streamflow is recharged by the increased meltwater from the accelerated
302 glacier retreat which may be partly stored in soil and aquifers in the wide and flat valley
303 (Figure 1b), and subsequently discharge into streams as baseflow.

304



305 **3.2. Variation of seasonal streamflow and its components**

306 The hydrograph of the Yangbajing catchment shows obvious intra-annual variation
307 (Figure 2). Streamflow sources and main components also change with the streamflow
308 magnitude. The variation trends of streamflow regimes also change across seasons. In
309 autumn, winter, and spring, both streamflow and baseflow show significant increasing
310 trends at least at the 5% level (Figures 7c, 7d and 7a). However, quickflow exhibits
311 nonsignificant trend for all seasons (Table 1). Streamflow increases significantly at the
312 5% level in autumn and the increasing trends reach the significant level of 1% in winter
313 and spring. Baseflow increases significantly at the 1% level in spring and autumn and
314 the increasing trend is at the 5% significance level in winter. However, the trends are
315 not statistically significant for both streamflow and its two components (quickflow and
316 baseflow) in summer (Figure 7b). As to the meteorological factors, mean air
317 temperature in all seasons increase significantly at the 1% level especially during winter
318 with the rate of about 0.51°C/10a (Table 1 and Figure 8), whereas precipitation in each
319 season shows nonsignificant trend during these years (Table 1).

320 Compared with monsoon rainfall as the main water source for summer which
321 accounts for about 73% of the total precipitation in the whole year, the corresponding
322 meltwater from glacier is considerable but its contribution to streamflow is limited.
323 Moreover, the summer meltwater and rainfall will partly infiltrate into soils and aquifers.
324 Carey and Quinton (2004) suggests that in snow and permafrost catchments with the
325 thin river valley and the steep slopes, meltwater infiltrates soils and resides in temporary



326 storage at the beginning of the melt period, and then are allowed to rapidly drain through
327 surface layers. However, due to thicker aquifers in the wide and flat catchment valley
328 (Figure 1b), summer meltwater and rainfall stored in aquifers are allowed to release
329 slowly from groundwater storage as baseflow in the following seasons, which has led
330 to the stability of baseflow in summer and the significant increase of baseflow in
331 autumn, winter and spring.

332 **3.3. Variation of baseflow recession rate and groundwater storage**

333 Using the data selected procedure mentioned in the section 2.3.3, we adopted daily
334 streamflow and precipitation records from September to December (the autumn and
335 early winter) over the period 1979-2013 in the catchment, during which the hydrograph
336 with little precipitation usually declines consecutively and smoothly. The fitted slope b
337 is equal to 1.79 through the non-linear least square fit of equation (10) for all data points
338 of $-dy/dt$ versus y in log-log space during the period 1979-2013. With the fixed slope
339 $b=1.79$, the recession coefficient K and groundwater storage S can be quantified by all
340 decades of the 1980s, 1990s and 2000s, and year-to-year from 1979 to 2013. For each
341 decade, the recession intercept a could be fitted by the fixed slope $b=1.79$. Then, the
342 values of K and m for each decade can be determined with the fitted recession intercept
343 a and the fixed slope b . And the groundwater storage S for each decade can be directly
344 estimated from the average rate of baseflow during recession period and the values of
345 K and m through equation (8). Meanwhile, the recession coefficient K and groundwater
346 storage S for each year can also be calculated according to the above procedure.



347 Figure 9 shows the non-linear least square fit of equation (10) to the plot of $-dy/dt$
348 versus y in log-log space for all recession data points of the observation records for each
349 decade of the 1980s, 1990s and 2000s, respectively. As shown in Figure 9, the recession
350 data points and fitted recession curves of each decade gradually move downward as
351 time goes on. It indicates that, with the fixed slope b , the recession intercept a gradually
352 decreases and recession coefficient K gradually increases. The values of recession
353 coefficient K for each decade are respectively $77 \text{ mm}^{0.79} \text{d}^{-0.21}$, $84 \text{ mm}^{0.79} \text{d}^{-0.21}$ and 103
354 $\text{mm}^{0.79} \text{d}^{-0.21}$ in the 1980s, 1990s and 2000s through recession flow analysis, which is
355 consistent with the results in Figure 9. Figure 10a shows the inter-annual variation of
356 recession coefficient K during the period 1979-2013. The recession coefficient K
357 increases slowly in the 1980s, fluctuates slightly in the 1990s and increases rapidly in
358 the 2000s. But its overall increasing trend is similar to the results obtained from decades
359 analysis. The trend of recession coefficient K shows significant increase at the 5% level
360 at a rate of about $7.70 (\text{mm}^{0.79} \text{d}^{-0.21})/10\text{a}$ from 1979 to 2013. This long-term variation
361 of recession coefficient K from September to December indicates that baseflow
362 recession process during autumn and early winter gradually slows down in the
363 catchment.

364 The mean values of groundwater storage S for each decade are 130 mm, 148 mm and
365 188 mm in the 1980s, 1990s and 2000s, respectively. The trend analysis suggests that
366 the groundwater storage S shows an increasing trend at the 5% significance level with
367 a rate of about $19.32 \text{ mm}/10\text{a}$ during the period 1979-2013 (Figure 10b). It indicates



368 that groundwater storage has been enlarged during autumn and early winter. The long-
369 term trend of groundwater storage S from 1979 to 2013 is consistent with the values
370 across decades. The inter-annual variation of groundwater storage S is also similar with
371 recession coefficient K (Figure 10a and 10b).

372 The increased groundwater storage S in autumn and early winter is associated with
373 the hypothesis that frozen ground degradation due to the significant rising air
374 temperature during autumn and winter (Figure 8c and 8d), which can enlarge
375 groundwater storage capacity (Niu et al., 2016). Figure 3 depicts the changes of surface
376 flow and groundwater flow paths in a glacier-fed and underlying-frozen ground
377 catchment under past climate and warmer climate, respectively. As frozen ground
378 extent continues to decline and active layer thickness continues to increase in the wide
379 and flat valley, the enlargement of groundwater storage capacity can provide enough
380 storage space to accommodate increasing meltwater, and support more meltwater to
381 percolate into deeper aquifers rather than surface layers, and thereby increase
382 groundwater storage in the valley floor (Figure 3). Then, the increase of groundwater
383 storage in autumn and earlier winter allows more groundwater discharge into streams
384 as baseflow, and lengthens the time scale of the baseflow recession process indicated
385 by recession coefficient K . This leads to increase baseflow and slow baseflow recession
386 processes in autumn and early winter, as is shown in Figure 7c, 7d and Figure 10a. In
387 the late winter and spring, the increase of baseflow (Figure 7d and 7a) can be explained
388 by the delayed release of increased groundwater storage.



389 **4. Conclusions**

390 In this study, the changes of hydro-meteorological variables were evaluated to
391 identify the main climatic factor for streamflow increase during the period 1979-2013
392 of the Yangbajain catchment, a sub-catchment with larger glacierization and large-scale
393 frozen ground in the Lhasa River basin in the south-central TP. We analyzed the changes
394 of streamflow components through baseflow separation method. We quantified
395 baseflow recession process and active groundwater storage in autumn and early winter
396 by recession flow analysis assuming nonlinearized outflow from aquifers into streams,
397 and analyzed the seasonal variations of streamflow and its components in response to
398 the changes in active groundwater storage.

399 We find that the increase of annual streamflow is mainly due to the increase of annual
400 baseflow, which is caused by increased temperature rather than precipitation in the
401 long-term period. The decreased glacial volume due to climate warming has supplied
402 large quantities of glacial meltwater which recharges aquifers and resides in temporary
403 storage during summer, and then releases as baseflow during the following seasons.
404 Moreover, the increase of active groundwater storage in autumn and early winter can
405 partly be attributed to the enlargement of groundwater storage capacity by frozen
406 ground degradation, which can provide storage spaces for increased glacial meltwater.
407 This can partly explain why baseflow volume increases and baseflow recession process
408 slows down in autumn, winter, and spring seasons.

409 This study provides a fundamental understanding of the changes in streamflow and



410 groundwater storage under warming climate. It is of great importance to predict the
411 effects of future climate changes on water resources and hydrological processes in
412 highly glacier-fed and large-scale frozen ground regions. Further analysis is needed to
413 quantify summer meltwater contribution to streamflow, and to explore the change of
414 groundwater storage capacity as frozen ground continues to degrade.

415 **Acknowledgements:**

416 This work was supported by the National Natural Science Foundation of China
417 (NSFC) (grants 91647108, 91747203), the Science and Technology Program of Tibet
418 Autonomous Region (2015XZ01432), and the Special Fund of the State Key
419 Laboratory of Hydrology-Water Resources and Hydraulic Engineering (no
420 20185044312).

421 **References**

- 422 Bayard, D., Stähli, M., Parriaux, A., and Flüeler, H.: The influence of seasonally frozen
423 soil on the snowmelt runoff at two alpine sites in southern Switzerland, *Journal of*
424 *Hydrology*, 309(1), 66-84, doi:10.1016/j.jhydrol.2004.11.012, 2005.
- 425 Bense, V. F., G. Ferguson., and H. Kooi.: Evolution of shallow groundwater flow
426 systems in areas of degrading permafrost, *Geophys. Res. Lett.*, 36, L22401,
427 doi:10.1029/2009GL039225, 2009.
- 428 Bense, V. F., Kooi, H., Ferguson, G., and Read, T.: Permafrost degradation as a control
429 on hydrogeological regime shifts in a warming climate, *Journal of Geophysical*
430 *Research Earth Surface*, 117, F03036, doi:10.1029/2011JF002143, 2012.
- 431 Bibi, S., Wang, L., Li, X. P., Zhou, J., Chen, D. L., and Yao, T. D.: Climatic and
432 associated cryospheric, biospheric, and hydrological changes on the Tibetan Plateau:



- 433 A review, *International Journal of Climatology*, 38, e1-e17, doi:10.1002/joc.5411,
434 2018.
- 435 Brutsaert, W.: Long-term groundwater storage trends estimated from streamflow
436 records: Climatic perspective, *Water Resources Research*, 44(2), 114-125,
437 doi:10.1029/2007WR006518, 2008.
- 438 Brutsaert, W., and Lopez, J. P.: Basin-scale geohydrologic drought flow features of
439 riparian aquifers in the southern Great Plains, *Water Resour. Res.*, 34(2), 233-240,
440 1998.
- 441 Brutsaert, W., and Nieber, J. L.: Regionalized drought flow hydrographs from a mature
442 glaciated plateau, *Water Resources Research*, 13(3), 637-643, 1977.
- 443 Buttle, J. M.: Mediating stream baseflow response to climate change: the role of basin
444 storage, *Hydrological Processes*, 32(1), doi:10.1002/hyp.11418, 2017.
- 445 Carey, S. K., and Quinton, W. L.: Evaluating snowmelt runoff generation in a
446 discontinuous permafrost catchment using stable isotope, hydrochemical and
447 hydrometric data, *Japanese Journal of Pharmacology*, 35, 309-324, 2004.
- 448 Chapman, T.: A comparison of algorithms for stream flow recession and baseflow
449 separation, *Hydrological Processes*, 13, 701-714, 1999.
- 450 Cheng, G. D., and Wu, T. H.: Responses of permafrost to climate change and their
451 environmental significance, Qinghai-Tibet Plateau, *Journal of Geophysical Research*
452 *Earth Surface*, 112, F02S03, doi:10.1029/2006JF000631, 2007.
- 453 Cuo, L., Zhang, Y. X., Zhu, F. X., and Liang, L. Q.: Characteristics and changes of
454 streamflow on the Tibetan Plateau: A review, *Journal of Hydrology Regional Studies*,
455 2, 49-68, doi:10.1016/j.ejrh.2014.08.004, 2014.
- 456 Duan, L., Man, X., Kurylyk, B.L., Cai, T.: Increasing winter baseflow in response to
457 permafrost thaw and precipitation regime shifts in northeastern China, *Water*, 9, 25,
458 doi:10.3390/w9010025, 2017.
- 459 Evans, S. G., and Ge, S.: Contrasting hydrogeologic responses to warming in



- 460 permafrost and seasonally frozen ground hillslopes, *Geophysical Research Letters*,
461 44, 1803-1813, doi:10.1002/2016GL072009, 2017.
- 462 Evans, S. G., Ge, S., and Liang, S.: Analysis of groundwater flow in mountainous,
463 headwater catchments with permafrost, *Water Resources Research*, 51, 9127-9140,
464 doi:10.1002/2014WR016259, 2015.
- 465 Evans, S. G., Ge, S., Voss, C. I., and Molotch, N. P.: The role of frozen soil in
466 groundwater discharge predictions for warming alpine watersheds, *Water Resources*
467 *Research*, 54, 1599-1615, 2018.
- 468 Gao, M., Chen, X., Liu, J., Zhang, Z., and Cheng, Q.: Using two parallel linear
469 reservoirs to express multiple relations of power-law recession curves, *Journal of*
470 *Hydrologic Engineering*, 04017013, doi:10.1061/(ASCE)HE.1943-5584.0001518,
471 2017.
- 472 Ge, S., J. McKenzie, C. Voss, and Wu, Q.: Exchange of groundwater and surface-water
473 mediated by permafrost response to seasonal and long term air temperature variation,
474 *Geophys. Res. Lett.*, 38, L14402, doi:10.1029/2011GL047911, 2011.
- 475 Green, T. R., Taniguchi, M., Kooi, H., Gurdak, J. J., Allen, D. M., and Hiscock, K. M.,
476 et al.: Beneath the surface of global change: impacts of climate change on
477 groundwater, *Journal of Hydrology*, 405(3), 532-560,
478 doi:10.1016/j.jhydrol.2011.05.002, 2011.
- 479 Immerzeel, W. W., van Beek, L. P. H., and Bierkens, M. F. P.: Climate change will affect
480 the Asian water towers, *Science*, 328, 1382-1385, 2010.
- 481 Jiang, W., Han, Z., Zhang, J., and Jiao, Q.: Stream profile analysis, tectonic
482 geomorphology and neotectonic activity of the Damxung-Yangbajain Rift in the
483 south Tibetan Plateau, *Earth Surface Processes & Landforms*, 41(10), 1312-1326,
484 doi:10.1002/esp.3899, 2016.
- 485 Kang, S. C., Xu, Y. W., You, Q. L., Flügel, W. A., Pepin, N., and Yao, T. D.: Review of
486 climate and cryospheric change in the Tibetan Plateau, *Environmental Research*



- 487 Letters, 5(1), 015101, doi:10.1088/1748-9326/5/1/015101, 2010.
- 488 Käser, D., and D. Hunkeler.: Contribution of alluvial groundwater to the outflow of
489 mountainous catchments, Water Resour. Res., 52, 680-697,
490 doi:10.1002/2014WR016730, 2016.
- 491 Kendall, M. G.: Rank Correlation Methods, 4th ed, Charles Griffin, London, pp. 196,
492 1975.
- 493 Kirchner, J.W.: Catchments as simple dynamical systems: catchment characterization,
494 rainfall-runoff modeling, and doing hydrology backward, Water Resources Research,
495 45, W02429, doi:10.1029/2008WR006912, 2009.
- 496 Lin, K. T., and Yeh, H. F.: Baseflow recession characterization and groundwater storage
497 trends in northern Taiwan, Hydrology Research, 48(6), 1745-1756, 2017.
- 498 Liu, J. S., Xie, J., Gong, T. L., Wang, D., and Xie, Y. H.: Impacts of winter warming
499 and permafrost degradation on water variability, upper Lhasa River, Tibet,
500 Quaternary International, 244(2), 178-184, doi:10.1016/j.quaint.2010.12.018, 2011.
- 501 Liu, J., Han, X., Chen, X., Lin, H., and Wang, A.: How well can the subsurface storage-
502 discharge relation be interpreted and predicted using the geometric factors in
503 headwater areas? Hydrological Processes, 30(25), 4826-4840,
504 doi:10.1002/hyp.10958, 2016.
- 505 Liu, X. D., and Chen, B.D.: Climatic warming in the Tibetan Plateau during recent
506 decades, International Journal of Climatology, 20(14), 1729-1742, 2000.
- 507 Lyne, V., and Hollick, M.: Stochastic time-variable rainfall-runoff modeling, Aust. Natl.
508 Conf. Publ. pp.89-93, 1979.
- 509 Lyon, S. W., and Destouni, G.: Changes in catchment-scale recession flow properties
510 in response to permafrost thawing in the Yukon River basin, International Journal of
511 Climatology, 30(14), 2138-2145, doi:10.1002/joc.1993, 2010.
- 512 Lyon, S. W., Destouni, G., Giesler, R., Humborg, C., Mörth, M., and Seibert, J., et al.:
513 Estimation of permafrost thawing rates in a sub-arctic catchment using recession



- 514 flow analysis, *Hydrology and Earth System Sciences Discussions*, 13(5), 595-604,
515 2009.
- 516 Mann, H.: Non-parametric test against trend, *Econometrica*, 13, 245-259, 1945.
- 517 Mi, D. S., Xie, Z. C., and Luo, X. R.: Glacier Inventory of China (volume XI: Ganga
518 River drainage basin and volume XII: Indus River drainage basin). Xi'an
519 Cartographic Publishing House, Xi'an, pp. 292-317 (In Chinese) , 2002.
- 520 Niu, L., Ye, B. S., Li, J., and Sheng, Y.: Effect of permafrost degradation on
521 hydrological processes in typical basins with various permafrost coverage in western
522 China, *Science China Earth Sciences*, 54(4), 615-624, doi:10.1007/s11430-010-
523 4073-1, 2011.
- 524 Niu, L., Ye, B., Ding, Y., Li, J., Zhang, Y., Sheng, Y., and Yue, G.: Response of
525 hydrological processes to permafrost degradation from 1980 to 2009 in the upper
526 Yellow River basin, China, *Hydrology Research*, 47(5), 1014-1024,
527 doi:10.2166/nh.2016.096, 2016.
- 528 Prasch, M., Mauser, W., and Weber, M.: Quantifying present and future glacier melt-
529 water contribution to runoff in a central Himalayan river basin, *Cryosphere*, 7(3),
530 889-904, doi:10.5194/tc-7-889-2013, 2013.
- 531 Pritchard, H. D.: Asia's glaciers are a regionally important buffer against drought,
532 *Nature*, 545(7653), 169, doi:10.1038/nature22062, 2017.
- 533 Qin, Y., Lei, H., Yang, D., Gao, B., Wang, Y., Cong, Z., and Fan, W.: Long-term change
534 in the depth of seasonally frozen ground and its ecohydrological impacts in the Qilian
535 Mountains, northeastern Tibetan Plateau, *Journal of Hydrology*, 542, 204-221, 2016.
- 536 Rupp, D. E., and Selker, J. S.: Information, artifacts, and noise in $dQ/dt-Q$ recession
537 analysis, *Adv. Water Res.*, 29(2), 154-160, 2006.
- 538 Singleton, M.J., and Moran, J.E.: Dissolved noble gas and isotopic tracers reveal
539 vulnerability of groundwater in a small, high elevation catchment to predicted
540 climate change, *Water Resour. Res.*, 46, W00F06, doi:10.1029/2009WR008718,



- 541 2010.
- 542 Smith, L. C., Pavelsky, T. M., Macdonald, G. M., Shiklomanov, A. I., Lammers, R. B.:
- 543 Rising minimum daily flows in northern Eurasian rivers: A growing influence of
- 544 groundwater in the high-latitude hydrologic cycle, *Journal of Geophysical Research*
- 545 *Biogeosciences*, 112, G04S47, doi:10.1029/2006JG000327, 2007.
- 546 St. Jacques, J. M. S., and Sauchyn, D. J.: Increasing winter base flow and mean annual
- 547 streamflow from possible permafrost thawing in the northwest Territories, Canada,
- 548 *Geophysical Research Letters*, 36(1), 329-342, doi:10.1029/2008GL035822, 2009.
- 549 Staudinger, M., Stoelzle, M., Seeger, S., Seibert, J., Weiler, M., and Stahl, K.:
- 550 Catchment water storage variation with elevation, *Hydrological Processes*, 31(11),
- 551 doi:10.1002/hyp.11158, 2017.
- 552 Viviroli, D., Du`rr, H. H., Messerli, B., Meybeck, M., and Weingartner, R.: Mountains
- 553 of the world, water towers for humanity: Typology, mapping, and global significance,
- 554 *Water Resour. Res.*, 43, W07447, doi:10.1029/2006WR005653, 2007.
- 555 Walvoord, M. A., and Kurylyk, B. L.: Hydrologic impacts of thawing permafrost-A
- 556 review, *Vadose Zone Journal*, 15(6), doi:10.2136/vzj2016.01.0010, 2016.
- 557 Walvoord, M. A., and Striegl, R. G.: Increased groundwater to stream discharge from
- 558 permafrost thawing in the Yukon River basin: Potential impacts on lateral export of
- 559 carbon and nitrogen, *Geophysical Research Letters*, 34(12), 123-134,
- 560 doi:10.1029/2007GL030216, 2007.
- 561 Wang, G., Mao, T., Chang, J., Song, C., and Huang, K.: Processes of runoff generation
- 562 operating during the spring and autumn seasons in a permafrost catchment on semi-
- 563 arid plateaus, *Journal of Hydrology*, 550, 307-317, 2017.
- 564 Wang, S., Liu, S. X., Mo, X. G., Peng, B., Qiu, J. X., Li, M. X., Liu, C. M., Wang, Z.
- 565 G., and Bauer-Gottwein, P.: Evaluation of remotely sensed precipitation and its
- 566 performance for streamflow simulations in basins of the southeast Tibetan Plateau,
- 567 *Journal of Hydrometeorology*, 16(6), 342-354, doi:10.1175/JHM-D-14-0166.1, 2015.



- 568 Wittenberg, H.: Baseflow recession and recharge as nonlinear storage processes,
569 Hydrological Processes, 13, 715-726, 1999.
- 570 Woo, M. K., Kane, D. L., Carey, S. K., and Yang, D.: Progress in permafrost hydrology
571 in the new millennium, Permafrost & Periglacial Processes, 19(2), 237-254,
572 doi:10.1002/ppp.613, 2008.
- 573 Wu, Q. B., and Zhang, T. J.: Recent permafrost warming on the Qinghai-Tibetan Plateau,
574 Journal of Geophysical Research Atmospheres, 113, D13108,
575 doi:10.1029/2007JD009539, 2008.
- 576 Wu, Z., and Zhao, X.: Quaternary geology and faulting in the Damxung-Yangbajain
577 Basin, southern Tibet, Journal of Geomechanics, 12(3), 305-316, 2006.
- 578 Yang, G., Lei, D., Hu, Q., Cai, Y., and Wu, J.: Cumulative coulomb stress changes in
579 the basin-range region of Gulu-Damxung-Yangbajain and their effects on strong
580 earthquakes, Electronic Journal of Geotechnical Engineering, 22(5), 1523-1530,
581 2017.
- 582 Yao, T. D., Pu, J. C., Lu, A. X., Wang, Y. Q., and Yu, W. S.: Recent glacial retreat and
583 its impact on hydrological processes on the Tibetan Plateau, China, and surrounding
584 regions, Arctic, Antarctic, and Alpine Research, 39(4), 642-650, 2007.
- 585 Yao, T. D., Wang, Y. Q., Liu, S. Y., Pu, J. C., Shen, Y. P., and Lu, A. X.: Recent glacial
586 retreat in high Asia in China and its impact on water resource in northwest China,
587 Science in China, 47(12), 1065-1075, doi:10.1360/03yd0256, 2004.
- 588 Yue, S., Pilon, P., Phinney, B., and Cavadias, G.: The influence of autocorrelation on
589 the ability to detect trend in hydrological series, Hydrological Processes, 16(9), 1807-
590 1829, doi:10.1002/hyp.1095, 2002.
- 591 Zhou, Y. W., Guo, D. X., Qiu, G. Q., Cheng, G. D., and Li, S. D.: Permafrost in China,
592 Science Press, Beijing, pp. 63-70 (In Chinese), 2000.
- 593 Zou, D., Zhao, L., Sheng, Y., and Chen, J., et al.: A new map of permafrost distribution
594 on the Tibetan Plateau, The Cryosphere, 11, 2527-2542, doi:10.5194/tc-11-2527-



595 2017, 2017.



Table 1. Mann-Kendall trend test with trend-free pre-whitening of seasonal and annual mean air temperature (°C), precipitation (mm), streamflow (mm), baseflow (mm) and quickflow (mm) from 1979 to 2013.

	Air temperature		Precipitation		Streamflow		Baseflow		Quickflow	
	Z _c	β (°C/a)	Z _c	β (mm/a)	Z _c	β (mm/a)	Z _c	β (mm/a)	Z _c	β (mm/a)
Spring	2.73**	0.026	0.90	0.290	3.05**	0.206	2.99**	0.147	0.98	0.042
Summer	2.63**	0.013	1.30	2.139	0.92	0.549	1.27	0.429	0.50	0.128
Autumn	2.65**	0.024	-0.68	-0.395	2.46*	0.546	2.96**	0.476	0.80	0.074
Winter	3.49**	0.051	-0.46	-0.014	3.08**	0.204	2.13*	0.145	1.39	0.016
Annual	4.48**	0.028	1.28	2.541	2.07*	1.230	2.70**	1.095	0.77	0.327

Comment: the symbols of asterisks *and ** mean statistically significant at the levels of 5% and 1%, respectively.



598 **Figure captions**

599 **Figure 1.** (a) The location, (b) elevation distribution, and (c) glacier and frozen ground
600 distribution (Zou et al., 2017) in the Yangbajain catchment of the Lhasa River basin in
601 the TP.

602 **Figure 2.** Seasonal variation of runoff depth (R), mean air temperature (T), and
603 precipitation (P) in the Yangbajain catchment.

604 **Figure 3.** Diagram depicting surface flow and groundwater flow due to glacier melt
605 and frozen ground thaw under (a) past climate and (b) warmer climate. Blue lines with
606 arrows are conceptual surface flow paths. Dark blue lines with arrows are conceptual
607 groundwater flow paths (after Evans and Ge. (2017)).

608 **Figure 4.** Variations of annual (a) runoff and (b) baseflow depth from 1979 to 2013.

609 **Figure 5.** Variations of annual (a) mean air temperature and (b) precipitation from 1979
610 to 2013.

611 **Figure 6.** The total area and volume of glaciers in the Yangbajain catchment in 1960
612 and 2009.

613 **Figure 7.** Variations of seasonal runoff and baseflow depth in (a) spring, (b) summer,
614 (c) autumn, and (d) winter from 1979 to 2013.

615 **Figure 8.** Variations of seasonal mean air temperature in (a) spring, (b) summer, (c)
616 autumn, and (d) winter from 1979 to 2013.

617 **Figure 9.** Recession data points of $-dy/dt$ versus y and fitted recession curves by decades
618 in log-log space. The black point line, dotted line, and solid line represent recession

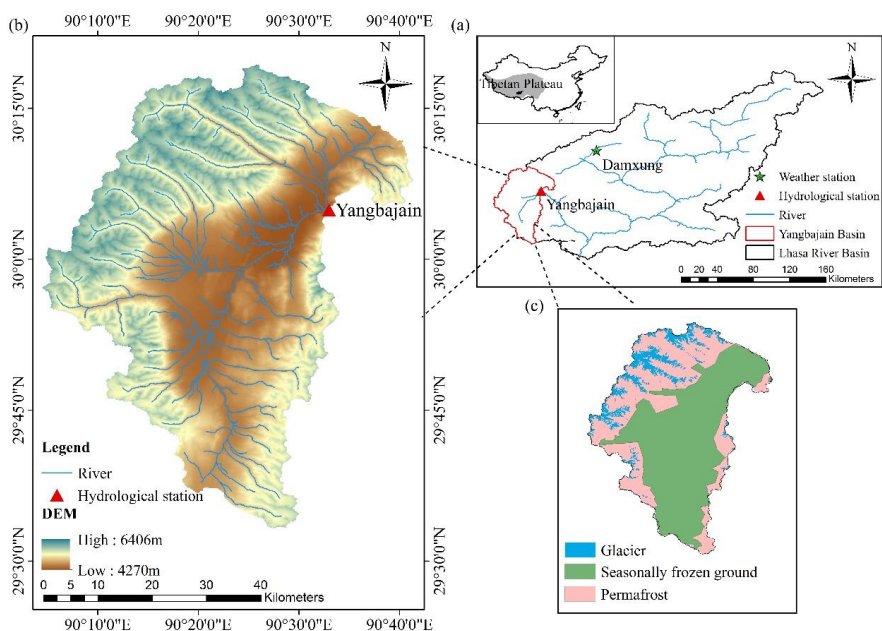


619 curves in the 1980s, 1990s, and 2000s, respectively.

620 **Figure 10.** Variations of (a) the recession coefficient K and (b) groundwater storage S

621 from 1979 to 2013.

622



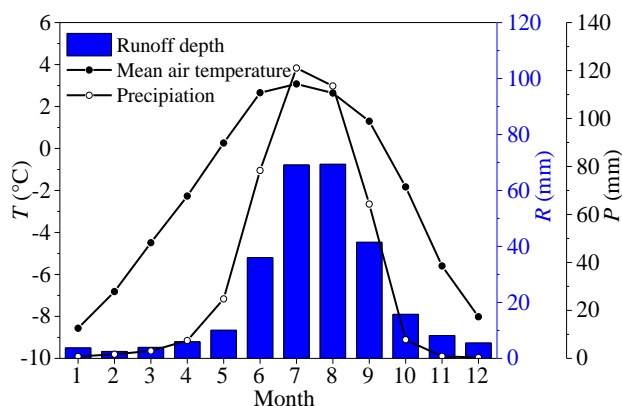
623

624 **Figure 1.** (a) The location, (b) elevation distribution, and (c) glacier and frozen ground

625 distribution (Zou et al., 2017) in the Yangbajain catchment of the Lhasa River basin in

626 the TP.

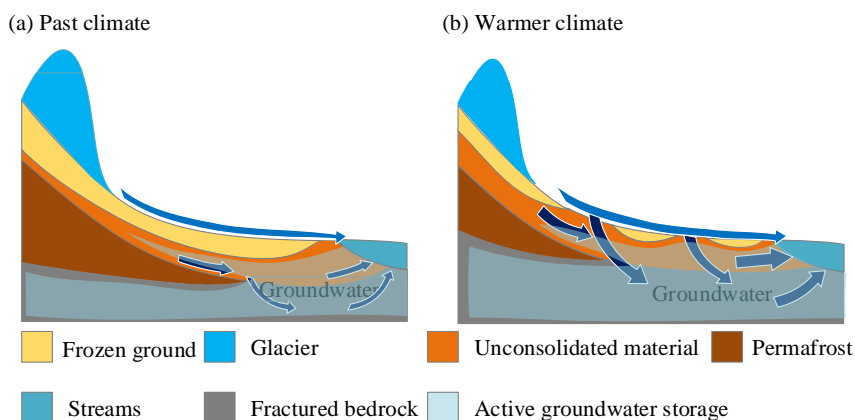
627



628

629 **Figure 2.** Seasonal variation of runoff depth (R), mean air temperature (T), and
 630 precipitation (P) in the Yangbajain catchment.

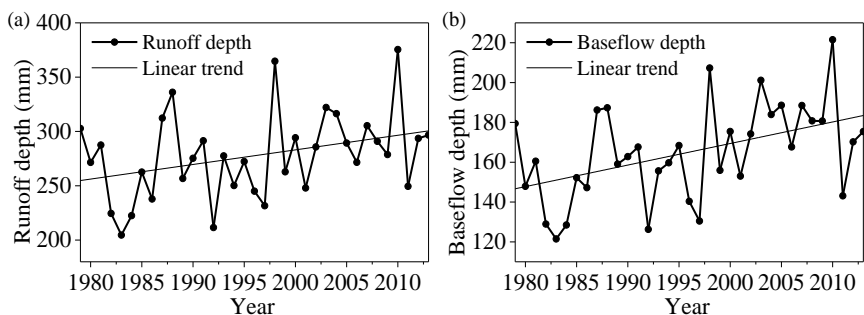
631



632

633 **Figure 3.** Diagram depicting surface flow and groundwater flow due to glacier melt
 634 and frozen ground thaw under (a) past climate and (b) warmer climate. Blue lines with
 635 arrows are conceptual surface flow paths. Dark blue lines with arrows are conceptual
 636 groundwater flow paths (after Evans and Ge. (2017)).

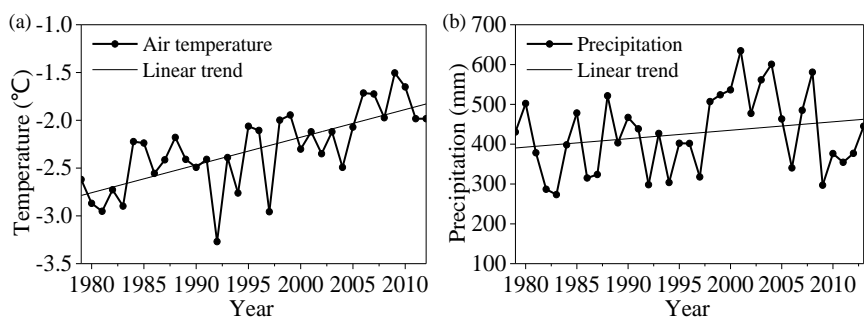
637



638

639 **Figure 4.** Variations of annual (a) runoff and (b) baseflow depth from 1979 to 2013.

640



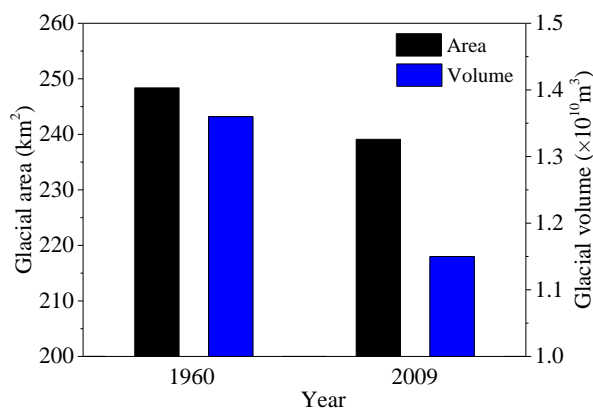
641

642 **Figure 5.** Variations of annual (a) mean air temperature and (b) precipitation from

643

1979 to 2013.

644



645

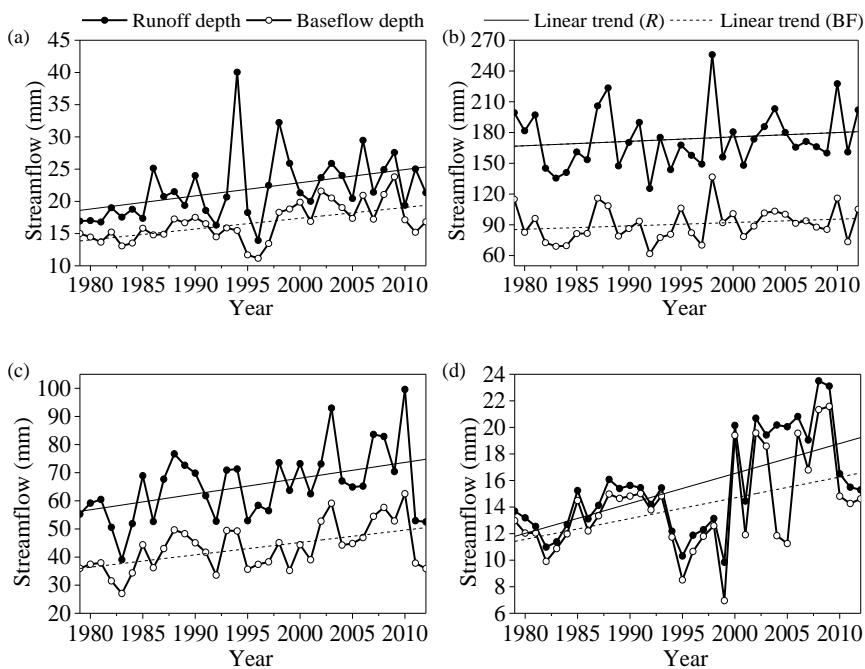
646

Figure 6. The total area and volume of glaciers in the Yangbajain catchment in

647

1960 and 2009.

648



649

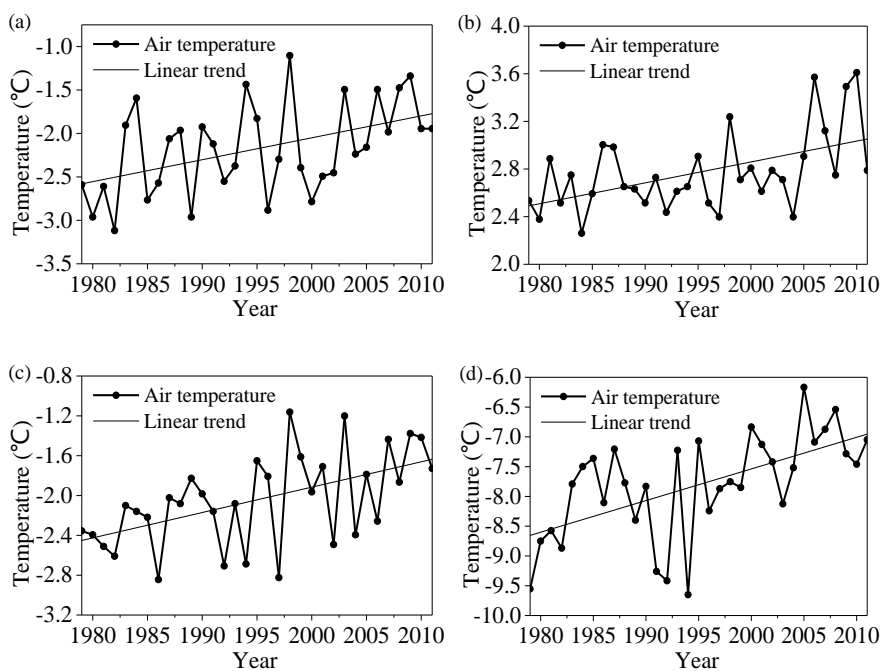
650

651

Figure 7. Variations of seasonal runoff and baseflow depth in (a) spring, (b)

652

summer, (c) autumn, and (d) winter from 1979 to 2013.



653

654

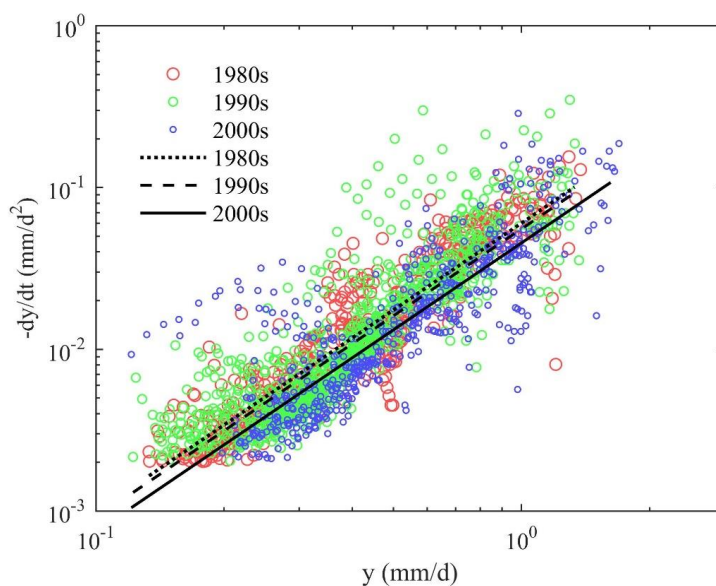
655

Figure 8. Variations of seasonal mean air temperature in (a) spring, (b) summer, (c)

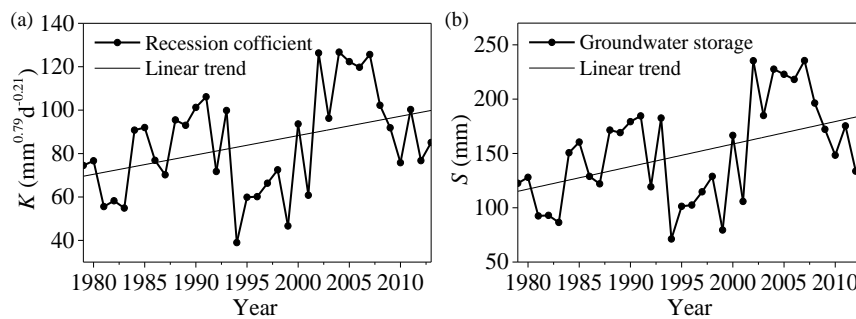
656

autumn, and (d) winter from 1979 to 2013.

657



658
 659 **Figure 9.** Recession data points of $-dy/dt$ versus y and fitted recession curves by decades
 660 in log-log space. The black point line, dotted line, and solid line represent recession
 661 curves in the 1980s, 1990s, and 2000s, respectively.
 662



663
 664 **Figure 10.** Variations of (a) the recession coefficient K and (b) groundwater storage
 665 S from 1979 to 2013.